Structure and Properties of Nitrile Rubber (NBR)–Clay Nanocomposites by Co-coagulating NBR Latex and Clay Aqueous Suspension

You-Ping Wu, Qing-Xiu Jia, Ding-Sheng Yu, Li-Qun Zhang

Key Laboratory for Preparation and Processing of Novel Polymer Materials, Beijing University of Chemical Technology, Beijing 100029, China

Received 16 September 2002; revised 2 January 2003; accepted 2 January 2003

ABSTRACT: Nitrile rubber (NBR)–clay nanocomposites were prepared by co-coagulating the NBR latex and clay aqueous suspension. Transmission electron microscopy showed that the silicate layers of clay were dispersed in the NBR matrix at the nano level and had a planar orientation. X-ray diffraction indicated that there were some nonexfoliated silicate layers in the NBR–clay nanocomposites. Stress–strain curves showed that the silicate layers generated evident reinforcement, modulus, and tensile strength of the NBR–clay nanocomposites, which were significantly improved with an increase in the amount of clay, and strain-at-break was higher than that of the gum NBR vulcanizate when the amount of clay was more than 5 phr. The NBR–clay nanocomposites exhibited an excellent gas barrier property; the reduction in gas permeability in the NBR–clay nanocomposites can be described by Nielsen's model. Compared with gum NBR vulcanizate, the oxygen index of the NBR–clay nanocomposites increased slightly. The feasibility of controlling rubber flammability via the nanocomposite approach needs to be evaluated further. © 2003 Wiley Periodicals, Inc. J Appl Polym Sci 89: 3855–3858, 2003

Key words: clay–nitrile rubber nanocomposites; structure; tensile strain–stress dependence; gas permeability; oxygen index

INTRODUCTION

Polymer–clay nanocomposites, especially plastic matrices, have attracted much attention recently, and these nanocomposites have been found to have outstanding mechanical properties, low gas permeabilities, and excellent fire-retardant properties.[1–6] But only a few studies of rubber–clay nanocomposites have been undertaken. Synthesis of rubber–clay nanocomposites has typically involved rubber melt or solution intercalation of organoclay, which has organic ammonium salts, or protonated amino-terminated polybutadiene/poly(butadiene-*co*-acrylonitrile) in the interlayer space.[7–10] A new approach for rubber matrices by the authors of this article, which was introduced in a patent,[11] involves mixing rubber latex and the clay aqueous suspension and co-coagulating by adding electrolytes, which is simpler and cheaper than the methods using organoclay. In our previous work the morphology and mechanical properties of styrene butadiene rubber (SBR) and carboxylated acrylonitrile butadiene(CNBR)–clay nanocomposites were investigated.[12–15] This report focuses on the structure and properties of nitrile rubber (NBR)–clay nanocomposites. The effect of different amounts of clay on the mechanical properties, gas permeability, and oxygen index of NBR–clay nanocomposites was studied in detail.

EXPERIMENTAL

Materials

The clay (Na-montmorillonite) used in this study, which had a cationic exchange capacity (CEC) of 93 mequiv/100 g, was from Liufangzi Clay Factory, Jilin, China. The NBR latex (AN 24%–26%) was from Lanzhou Petrochemical Company (China). The silica (Hi-Sil-255N) came from the Jiangxi Nanji Silica factory (Nanchang, China).

Preparation of NBR–clay nanocomposites

The clay aqueous suspension, the NBR latex, and the compatibilizer were mixed and vigorously stirred for a given period of time. Then this mixture was coagulated in the electrolyte solution, washed with water, and dried in oven for 18 h at 80°C.

Correspondence to: L. Zhang (zhangliqunghp@yahoo.com).
Contract grant sponsor: National Natural Science Foundation of China; contract grant number: 05173003.
Contract grant sponsor: Beijing New Star plan project; contract grant number: H010410010112.

© 2003 Wiley Periodicals, Inc.

TABLE I
Compositions (phr)

NBR	100
Filler	0, 3, 5, 10, 15, 20, 25, 30
Zinc oxide	5.0
Stearic acid	1.0
Accelerator DM	1.0
Sulfur	1.5
Antioxidant 4010NA	2.0

Compounding and vulcanization

The compositions are shown in Table I. The compounds were prepared with a 6-in. two-roll mill and were vulcanized in a standard mold at 160°C for t_{90}.

Characterization

Transmission electron microscopy (TEM) micrographs were taken from ultrathin sections with an H-800 TEM, using an acceleration voltage of 200 KV. X-ray diffraction (XRD) analyses were carried out on a Rigaku RINT using Cu Kα radiation, a 0.02°C step size, and 6.00° at 2θ/min. Tensile testing were performed according to Chinese Standard GB 528-98 at 30 mm/min. The nitrogen permeation experiment was carried out with a gas permeability–measuring apparatus. The pressure on one face of the sheet (about 1 mm thick) was kept at 0.57 MPa and the other initially at zero pressure, and the nitrogen permeated through the sheet. The rate of nitrogen transmission at 40°C was obtained by gas chromatography, and the nitrogen permeability was calculated from that.

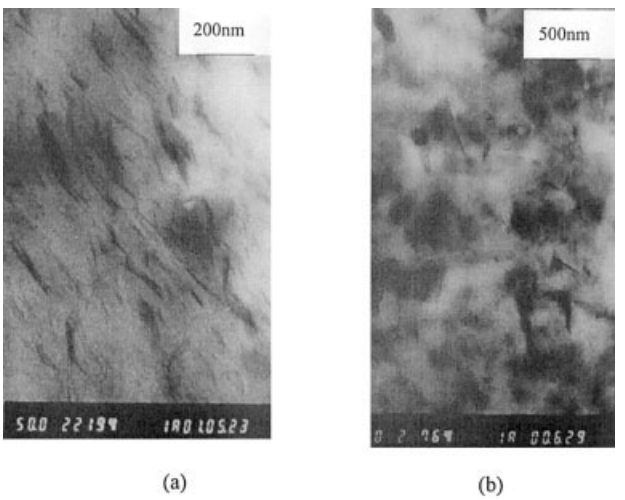

Figure 1 TEM photographs of NBR–clay nanocomposite containing 20 phr of clay in different directions: (a) longitudinal; (b) vertical.

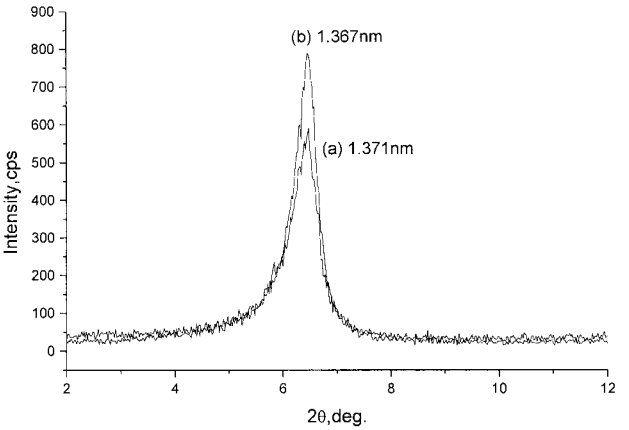

Figure 2 XRD patterns of NBR–clay nanocomposites. NBR–clay (w/w): (a) 100:10; (b) 100:20.

RESULTS AND DISCUSSION

Morphology

TEM micrographs of the NBR–clay nanocomposite containing 20 phr of clay in different directions are shown in Figure 1. The dark lines in Figure 1(a) are the intersections of the silicate layers. As seen in Figure 1(a), silicate layers were exfoliated and dispersed in the NBR matrix at the nano level, and the thickness of most silicate layers was about 3–5 nm and the width about 100–200 nm. The dark areas in Figure 1(b) are the intersections of the silicate layers. From comparing it to Figure 1(a), it can be seen that the silicate layers in Figure 1(b) have a planar orientation parallel to the surface in the specimen.

The XRD patterns of the NBR–clay nanocomposites with different clay loading levels are presented in Figure 2, where peaks correspond to the (001) plane reflections of the clay. This result indicates the existence of some nonexfoliated silicate layers, which are evident in Figure 1(a), with a thickness of less than 20 nm. In addition, the amount of nonexfoliated layers increased with growth of the clay content.

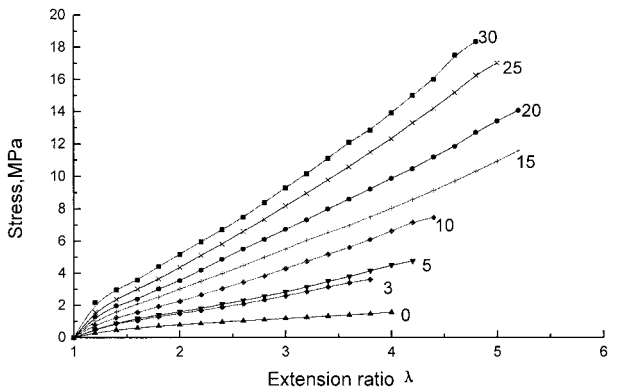

Figure 3 Stress–strain of NBR–clay nanocomposites with varied clay content (indicated, phr).

TABLE II
Nitrogen Permeabilities of NBR–clay Nanocomposites (10^{-17} m^2 pa^- s^{-1})[a]

Filler content, phr	0	10	20	30
Silica volume fraction, %	0	4.41	8.44	12.15
Clay volume fraction, %	0	3.59	6.93	10.05
Silica	1.67	1.51	1.33	1.27
Clay	1.67	1.17	0.97	0.85

Silica ρ = 2.1 g/cm^3; clay ρ = 2.6 g/cm^3; NBR ρ = 0.968 g/cm^3

Effect of clay content on properties of NBR–clay nanocomposites

Stress–strain curves for NBR–clay nanocomposites with various clay contents are given in Figure 3, from which it is clear that modulus and tensile strength were significantly improved with an increase in the filled amount of clay. The tensile strength of the nanocomposite filled with 30 phr of clay was about 10 times greater than that of the gum NBR vulcanizate. When the filled amount of clay was more than 5 phr, strain-to-break was higher than that of the gum NBR vulcanizate. The large improvement in the ultimate properties is a result of the dispersed structure of clay at the nano level and the planar orientation of the silicate layers.

The gas permeabilities of gum NBR vulcanizate, NBR–clay nanocomposites, and NBR filled with silica are presented in Table II, which shows that nitrogen permeability was reduced with an increase in the amount of filler and that the NBR–clay nanocomposites had a better gas barrier property than did the NBR filled with the same amounts of silica. This can be attributed to the impermeable filler phase and the large aspect ratio of the silicate layers. Compared with the gum NBR vulcanizate, the nitrogen permeability of the NBR–clay nanocomposites with 10, 20, and 30 phr of clay was reduced by 29%, 41%, and 48%, respectively. It can be concluded that having silicate layers with a large aspect ratio and a planar orientation leads to a great increase in the diffusion distance by creating a tortuous path for the diffusing gas.

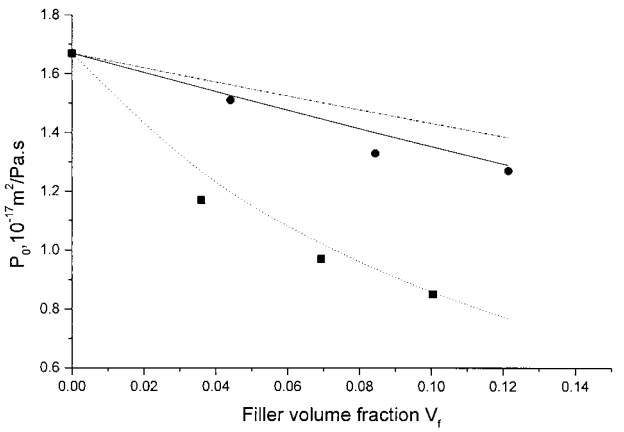

Figure 4 Effect of filler volume fraction (V_f) on nitrogen permeability: eq. (1); eq. (2) α = 1; eq. (2) α = 15; ● silica; ■ clay.

TABLE III
Oxygen Index of NBR–Clay Nanocomposites (%)

Filler content, phr	0	10	20	30
Silica	18.4	19.2	19.5	20.7
Clay	18.4	19.0	20.2	21.2

In Figure 4, the full line shows the permeability, P, of nitrogen in the composite calculated from the equation:[16]

$$P = P_0 (1 - V_f)^2 \quad (1)$$

where P_0 is the permeability of nitrogen in gum NBR vulcanizate and V_f is the volume fraction of filler. In eq. (1) the solubility coefficient and diffusion coefficient are assumed to be proportional to the volume fraction of filler. The permeability in NBR filled with silica can be described by eq. (1). However, in NBR–clay nanocomposites the permeability values were lower than those calculated by eq. (1), apparently because eq. (1) neglects particle shape and orientation, which are the important factors influencing the diffusion coefficient.

The Nielsen model[17] was also used to estimate the permeability in a system filled with platelets of aspect ratio α aligned parallel to the surface:

$$P = P_0 (1 - V_f)/(1 + V_f \alpha/2) \quad (2)$$

where P_0 is the permeability of the sample without the filler. For impermeable spheres using eq. (2), in which α = 1, is well justified for small filler loading. The fit of eq. (2) to the data of the NBR–clay nanocomposites is represented by the dotted line in Figure 4. The result was similar to the air permeability of an intercalated clay/acrylonitrile–butadiene copolymer nanocomposite prepared by melt intercalation.[18] As seen from Figure 4, the fit resulted in an effective aspect ratio of 15, lower than the value of 37 estimated by TEM micrographs, which may be because the Nielsen model considers geometrical impedance of a single particle and the longest path for the diffusing gas, but neglects their mutual diffusion back scattering.[19] This aspect of the detailed research is in progress and will be reported in other articles. In addition, the dashed and dotted line shows the nitrogen permeability obtained from eq. (2) with α = 1, which is a little higher than that of NBR filled with silica.

The oxygen index of the NBR–clay nanocomposites is shown in Table III, with gum NBR vulcanizate and NBR filled with the same amounts of silica used as

references. The oxygen index increased slightly with an increase in the amount of filler, but no differences were noticeable between the NBR–clay nanocomposites and NBR with silica. These results are similar to those found for the polypropylene system.[20] However, Gilman and Kashiwagi[4] found that the peak heat release rate (HRR) was reduced by 63% in a nylon-6 clay nanocomposite containing only 5 wt % clay. The low flammability of polymer–-clay nanocomposites originates in the formation of a clay-reinforced carbonaceous char during combustion of the nanocomposites that may act as an excellent insulator and a mass transport barrier, slowing the escape and transport of the volatile products into the gas phase. Unfortunately, for nanocomposites, an initially higher HRR and a shorter ignition time also were observed, and so they did not pass the UL-94 flammability test.[21] Whether the clay–nanocomposite approach is efficient for clay–rubber systems is an interesting subject, and the fire-retardant mechanism needs to be investigated further.

CONCLUSIONS

In the NBR–clay nanocomposites prepared by cocoagulating the NBR latex and clay aqueous suspension, the silicate layers of clay were dispersed in the NBR matrix at the nano level and had a planar orientation. NBR–clay nanocomposites exhibited excellent mechanical and gas barrier properties, which can be described by Nielsen's model. The oxygen index of NBR–clay nanocomposites increased slightly compared with that of the gum NBR vulcanizate. The feasibility of controlling rubber flammability via the nanocomposite approach still needs further evaluation. It seems that this new material can be applied in rubber products, such as the inner tube, inner liner, and dumper.

References

1. Kojima, Y.; Usuki, A.; Kawasumi, M.; Okada, A.; Kurauchi, T.; Kamigaito, O. J Appl Polym Sci 1993, 49, 1259.
2. Messersmith, P. B.; Giannelis, E. P. J Polym Sci, Part A: Polym Chem 1995, 33, 1047.
3. Giannelis, E. P. Adv Mater 1996, 8, 29.
4. Gilman, J. W.; Kashiwagi, T. SAMPE J 1997, 33, 40.
5. Vaia, R. A.; Price, G.; Ruth, P. N.; Nguyen, H. T; Lichtenhan, J. Appl Clay Sci 1999, 15, 67.
6. Liu, T. M; Baker, W. E.; Langille, K. B.; Nguyen, D. T.; Bernt, J. O. J Vinyl Additive Technol 1998, 4, 246.
7. Wang, S. J.; Long, C. F.; Wang, X. Y.; Li, Q.; Qi, Z. N. J Appl Polym Sci 1998, 69, 1557.
8. Kojima, Y.; Fukumori, K.; Usuki, A.; Okada, A.; Kurauchi, T. J Mater Sci Lett 1993, 12, 889.
9. Ganter, M.; Gronski, W.; Semke, H.; Zilg, T.; Thomann, C.; Muhlhaupt, R. Kautschuk Gummi Kunstoffe 2001, 54, 166.
10. Moet, A.; Akelah, A.; Salahuddin, N.; Hiltner, A.; Baer, E. Proc Mater Res Soc, San Francisco, Apr 2–8, 1994.
11. Zhang, L. Q.; Wang, Y. Z.; Yu, D. S.; Wang, Y. Q.; Sun, Z. H. CNZL 98 1 01496.8, 2002.
12. Wu, Y. P.; Zhang, L. Q.; Wang, Y. Q.; Liang, Y.; Yu, D. S. J Appl Polym Sci 2001, 82, 2842.
13. Zhang, L. Q.; Wang, Y. Z.; Wang, Y. Q.; Sui, Y.; Yu, D. S. J Appl Polym Sci 2000, 78, 1873.
14. Wang, Y. Z.; Zhang, L. Q.; Tang, C. H.; Yu, D. S. J Appl Polym Sci 2000, 78, 1879.
15. Wu, Y. P.; Zhang, L. Q.; Wang, Y. Z.; Wang, Y. Q.; Sun, Z. H.; Zhang, H. F.; Yu, D. S. Chinese J Mater Res 2000, 14, 188.
16. Crank, J.; Park, G. S.; Eds. Diffusion in Polymer; Academic Press: New York, 1968; p 214.
17. Nielsen, L. E. J Macromol Sci 1967, A15, 929.
18. Nah, C.; Ryn, H. J.; Kim, W. D.; Choi, S. S. Polym Adv Technol 2002, 13, 649.
19. Sekelik, D. J.; Stepanov, E. V.; Nazarenko, S.; Schiraldi, D.; Hiltner, A.; Baer, E. J Polym Sci, Part B: Polym Phys 1999, 37, 847.
20. Le Bras, M.; Bourbigot, S. Fire Mater 1996, 20, 39.
21. Morgan, A; Gilman, J. W. Proceedings; Fire Retardant Chemicals Association: Washington DC, 2000; p 25–39.